JACS
JOURNAL OF THE AMERICAN CHEMICAL SOCIETY
Article
pubs.acs.org/JACS

Unraveling the Structure–Affinity Relationship between Cucurbit[*n*]urils (*n* = 7, 8) and Cationic Diamondoids

David Sigwalt,[†] Marina Šekutor,[‡] Liping Cao,[†] Peter Y. Zavalij,[†] Jiří Hostaš,[§] Haresh Ajani,[§,∥] Pavel Hobza,[*,§,∥] Kata Mlinarić-Majerski,[*,‡] Robert Glaser,[*,⊥] and Lyle Isaacs[*,†]

[†]Department of Chemistry and Biochemistry, University of Maryland, College Park, Maryland 20742, United States
[‡]Department of Organic Chemistry and Biochemistry, Ruđer Bošković Institute, Bijenička cesta 54, 10000 Zagreb, Croatia
[§]Institute of Organic Chemistry and Biochemistry, Academy of Sciences of the Czech Republic, 16610 Praha 6, Czech Republic
[∥]Regional Center of Advanced Technologies and Materials, Department of Physical Chemistry, Palacký University, 77146 Olomouc, Czech Republic
[⊥]Department of Chemistry, Ben-Gurion University of the Negev, Beer-Sheva 84105, Israel

Supporting Information

ABSTRACT: We report the measurement of the binding constants (K_a) for cucurbit[*n*]uril (*n* = 7, 8) toward four series of guests based on 2,6-disubstituted adamantanes, 4,9-disubstituted diamantanes, 1,6-disubstituted diamantanes, and 1-substituted adamantane ammonium ions by direct and competitive ^{1}H NMR spectroscopy. Compared to the affinity of CB[7]·Diam$(NMe_3)_2$, the adamantane diammonium ion complexes (e.g., CB[7]·2,6-Ad$(NH_3)_2$ and CB[7]·2,6-Ad$(NMe_3)_2$) are less effective at realizing the potential 1000-fold enhancement in affinity due to ion–dipole interactions at the second ureidyl C═O portal. Comparative crystallographic investigation of CB[7]·Diam$(NMe_3)_2$, CB[7]·DiamNMe$_3$, and CB[7]·1-AdNMe$_3$ revealed that the preferred geometry positions the $^+$NMe$_3$ groups ≈0.32 Å above the C═O portal; the observed 0.80 Å spacing observed for CB[7]·Diam$(NMe_3)_2$ reflects the simultaneous geometrical constraints of $CH_2\cdots O{=}C$ close contacts at both portals. Remarkably, the CB[8]·IsoDiam$(NHMe_2)_2$ complex displays femtomolar binding affinity, placing it firmly alongside the CB[7]·Diam$(NMe_3)_2$ complex. Primary or quaternary ammonium ion looping strategies lead to larger increases in binding affinity for CB[8] than for CB[7], which we attribute to the larger size of the carbonyl portals of CB[8]; this suggests routes to develop CB[8] as the tightest binding host in the CB[*n*] family. We report that alkyl group fluorination (e.g., CB[7]·1-AdNH_2Et versus CB[7]·1-Ad$NH_2CH_2CF_3$) does not result in the expected increase in K_a value. Finally, we discuss the role of solvation in nonempirical quantum mechanical computational methodology, which is used to estimate the relative changes in Gibbs binding free energies.

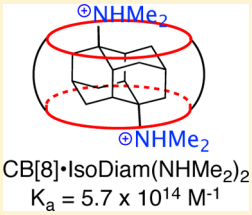

INTRODUCTION

The development of receptor·ligand pairs that are simultaneously high affinity, highly selective, and stimuli responsive is an important goal in both chemical and biotechnology applications. For example, biotin·avidin technology has been used for protein and nucleic acid purification, enzyme linked immunosorbent assays, and immobilization of biomolecules on solid phases.[1] The discovery of new purely synthetic high affinity aqueous host·guest pairs[2] allows for an expansion of the range of applications and, equally importantly, allows a determination of the fundamental factors governing noncovalent interactions in water. The cucurbit[*n*]uril (CB[*n*], *n* = 5, 6, 7, 8, 10, 14; Chart 1) family of molecular containers comprises *n* glycoluril rings connected by 2*n* methylene bridges.[3] The ureidyl carbonyl groups define two symmetry equivalent C═O portals that possess a highly negative electrostatic potential and that guard entry to a hydrophobic cavity.[4] In pioneering work, Mock showed that guests that contain both a cationic unit (e.g., ammonium) and a hydrophobic unit bind with high affinity and selectivity toward CB[6] in acidic aqueous solution.[5] For example, CB[6] binds to spermine with $K_a = 1.3 \times 10^7$ M^{-1} by a combination of ion–dipole interactions and the hydrophobic effect (Chart 1). In 2005, we discovered that CB[7] exhibits ultra high affinity toward adamantane derivatives (e.g., 1-AdNH$_3$, $K_a = 4.2 \times 10^{12}$ M^{-1}), as measured by ^{1}H NMR competition experiments.[6] Subsequently, several groups investigated adamantane, ferrocene, bicyclo[2.2.2]octane, and dodecaborane as scaffolds[7] to support dications, but the highest affinity achieved was for the CB[7]·1-Ad$NH_2(CH_2)_2NH_3$ complex ($K_a = 5 \times 10^{15}$ M^{-1} in unbuffered water; $K_a = 2.4 \times 10^{13}$ M^{-1} in 50 mM NaOAc buffered D_2O, pH 4.74), wherein only one C═O portal

Chart 1. Structure of CB[*n*] Molecular Containers

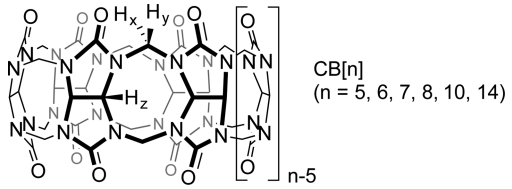

Received: January 3, 2017
Published: February 9, 2017

DOI: 10.1021/jacs.7b00056
J. Am. Chem. Soc. 2017, 139, 3249–3258

engages in ion−dipole interactions. Recently, Nau, Scherman, and co-workers reported that one source of the high affinity of CB[7]·guest complexes is the high energy H_2O molecules bound within uncomplexed CB[7] that are released upon formation of CB[7]·guest complexes.[8] Given that ion−dipole (ammonium···O═C) interactions constitute a major driving force toward CB[n]·guest complexation, we surmised that further improvements in CB[7]·guest affinities would be possible if we could introduce ion−dipole interactions at the second ureidyl C═O portal. In 2014, we reported our initial investigation of the diamantane scaffold and disclosed that CB[7] and Diam$(NMe_3)_2$ (Chart 2) form a spectacularly tight

Chart 2. Structure of the Guests Used in This Study

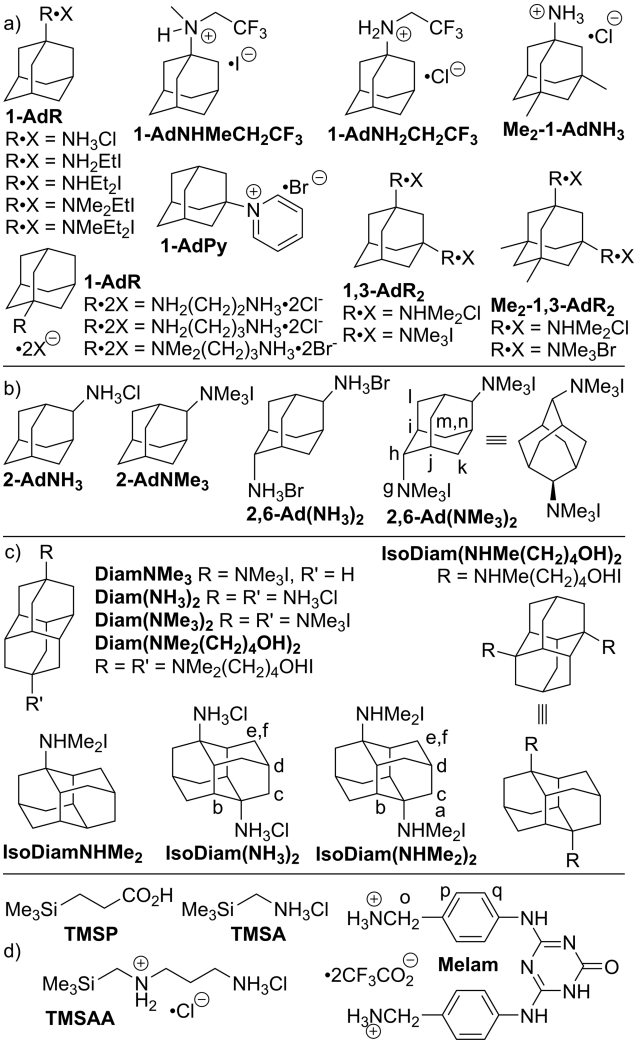

complex ($K_a = 7.2 \times 10^{17}$ M^{-1} in D_2O; $K_a = 2 \times 10^{15}$ M^{-1} in 50 mM NaOAc buffered D_2O, pH 4.74) in aqueous solution.[9] Subsequently, we investigated 2,6-bis(trimethylammonio)-naphthalene, which has a similar spacing (≈ 7.8 Å) between NMe_3 groups but a different hydrophobic scaffold; this highlighted the importance of the more hydrophobic diamantane scaffold.[10] Recently, we have also validated the use of DFT calculations to reproduce the binding affinities and geometries of known ultratight complexes and to predict others.[11] In this article, we provide a full account of our studies of the binding of CB[7] and CB[8] toward guests based on the adamantane and diamantane scaffolds.

RESULTS AND DISCUSSION

This section is organized as follows. First, we describe the design and synthesis of new guests. Next, we verify the 1:1 nature of the host−guest complexes and describe the measurement of their binding constants by direct or competition ^{1}H NMR measurements. Finally, we discuss the trends in the K_a values supplemented by information on the host−guest geometries gleaned from their X-ray crystal structures and binding energy subcomponents calculated using energy decomposition analysis (EDA). We have calculated correlation (ρ^2 = 0.68) between 20 experimental (ΔG_{explt}) and calculated changes of Gibbs binding free energies (ΔG_{calcd}) that can be found in Figure S1 in the Supporting Information.

Design and Synthesis of Guests. The structures of guests used in this study are shown in Chart 2. Initially, we sought to reach higher levels of affinity within the adamantane series by creating diammonium ions in which both C═O portals are occupied. For this purpose, we selected dicationic 2,6-disubstituted adamantanes (e.g., 2,6-AdR_2), which possess a five carbon atom spacing between N atoms; this is known to complement the spacing between C═O portals in CB[n] hosts.[12] We also studied the corresponding monoammonium compounds (2-AdR, Chart 2b) as monocationic controls. As described previously, 4,9-disubsituted diamantane derivative Diam$(NMe_3)_2$ forms a remarkably tight complex with CB[7].[9] To further define the factors governing this high affinity binding, we investigated the binding of additional mono- and dicationic derivatives of diamantane (DiamNMe_3 and DiamR_2; IsoDiam$NHMe_2$ and IsoDiamR_2) toward CB[7] and CB[8]. The Diam and IsoDiam compounds (Chart 2c) differ in the number of C atoms between N atoms (six for DiamR_2 and four for IsoDiamR_2) and also in the disposition of their steric bulk. Within these series, we also studied the influence of the cation (e.g., NH_3 versus NMe_3 or $NHMe_2$). Within the series of compounds that contain ammoniums at the 1-position of adamantane (Chart 2a) are compounds that probe the influence of degree of alkylation (e.g., 1-AdR), the presence of a second ammonium ion in the form of a loop (e.g., 1-Ad$NMe_2(CH_2)_3NH_3$), the influence of electrostatics (e.g., 1-Ad$NH_2CH_2CF_3$), and the effects of steric bulk (e.g., Me_2-1,3-AdR_2). Chart 2d shows the structures of the compounds used as competitors of known K_a in the binding constant determinations by ^{1}H NMR competition experiments.[6,9,10]

The majority of guest compounds used in this article are either commercially available or have been synthesized as reported previously.[3e,6,9,11,13] The synthesis of all new guests is described in detail in the Supporting Information. For example, DiamNMe_3, IsoDiam$NHMe_2$, and 2-AdNMe_3 were prepared by the alkylation of the corresponding amines with MeI in good yield. Similarly, 1-AdNH_2Et, 1-AdNMe_2Et, 1-Ad$NHEt_2$, and 1-Ad$MeEt_2$ were prepared by the stepwise alkylations of 1-AdNH_2 with EtI and MeI. Finally, compounds 1-Ad$NH_2CH_2CF_3$ and 1-Ad$NHMeCH_2CF_3$ were prepared by acylation of 1-AdNH_2 with trifluoroacetic anhydride, reduction with $LiAlH_4$, and alkylation with MeI.

Selection of Buffer. CB[n]·guest complexes have been studied in a wide variety of solvents including pure water, aq. HCO_2H, NaOAc buffered water, and sodium phosphate buffered water.[5,6,14] It is known from the literature that CB[n] binds alkali metal cations (Li^+, Na^+, K^+) at their ureidyl C═O portals and that this competitive binding reduces the

DOI: 10.1021/jacs.7b00056
J. Am. Chem. Soc. 2017, 139, 3249−3258

observed K_a values of CB[n] toward other guests.[15] For this reason, both pH and metal ion concentration must be carefully controlled to allow comparison between measured K_a values. Accordingly, we used 50 mM NaOAc buffered D_2O (pH 4.74), which we used previously in related ^{1}H NMR competition experiments.[6,9,10]

Investigation of the Nature of the Complexes between CB[7] or CB[8] and the Various Guests. Before proceeding to the ^{1}H NMR competition experiments to determine K_a values for the host·guest complexes, we verified their 1:1 nature and elucidated their geometrical features.[6] We illustrate this process for two of our tightest binding complexes, namely, CB[7]·2,6-Ad(NMe_3)$_2$ and CB[8]·IsoDiam($NHMe_2$)$_2$. Figure 1a–c shows the ^{1}H NMR spectra recorded for 2,6-

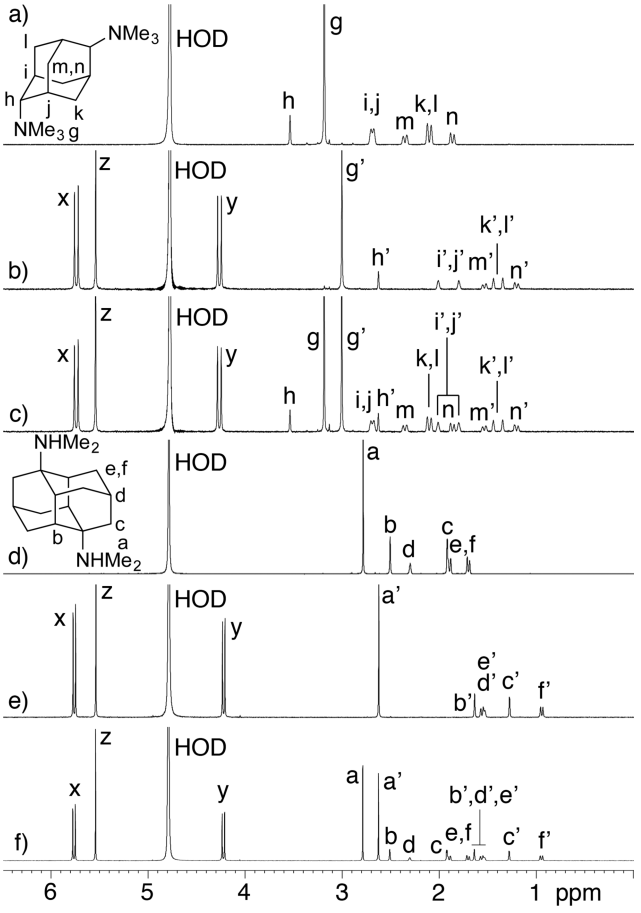

Figure 1. ^{1}H NMR spectra recorded (400 MHz (a–c) or 600 MHz (d–f), D_2O, RT) for (a) 2,6-Ad(NMe_3)$_2$ (0.25 mM), (b) CB[7]·2,6-Ad(NMe_3)$_2$ (0.25 mM), (c) a mixture of CB[7]·2,6-Ad(NMe_3)$_2$ (0.25 mM) and 2,6-Ad(NMe_3)$_2$ (0.25 mM), (d) IsoDiam($NHMe_2$)$_2$ (0.25 mM), (e) CB[8]·IsoDiam($NHMe_2$)$_2$ (0.25 mM), and (f) a mixture of CB[8]·IsoDiam($NHMe_2$)$_2$ (0.25 mM) and IsoDiam($NHMe_2$)$_2$ (0.25 mM). Primed (′) resonances arise from CB[n]·guest complex.

Ad(NMe_3)$_2$ alone, CB[7]·2,6-Ad(NMe_3)$_2$, and CB[7]·2,6-Ad(NMe_3)$_2$ in the presence of excess free 2,6-Ad(NMe_3)$_2$. Figure 1c shows that CB[7]·2,6-Ad(NMe_3)$_2$ undergoes slow exchange with free 2,6-Ad(NMe_3)$_2$ on the chemical shift time scale; integration of resonances for bound 2,6-Ad(NMe_3)$_2$ versus CB[7] within CB[7]·2,6-Ad(NMe_3)$_2$ establishes the 1:1 nature of the host·guest complex. Figure 1b shows that the seven symmetry nonequivalent protons (H_h–H_n) of the adamantane core of 2,6-Ad(NMe_3)$_2$ undergo sizable upfield shifts upon complexation, which is consistent with their binding in the cavity of CB[7].[12,16] The NMe_3 H_g resonance also shifts upfield but less dramatically, which reflects its location in the bond–dipole region near the portals (vide infra).[8a]

Figure 2d–f shows the ^{1}H NMR spectra recorded for IsoDiam($NHMe_2$)$_2$ alone, the CB[8]·IsoDiam($NHMe_2$)$_2$ com-

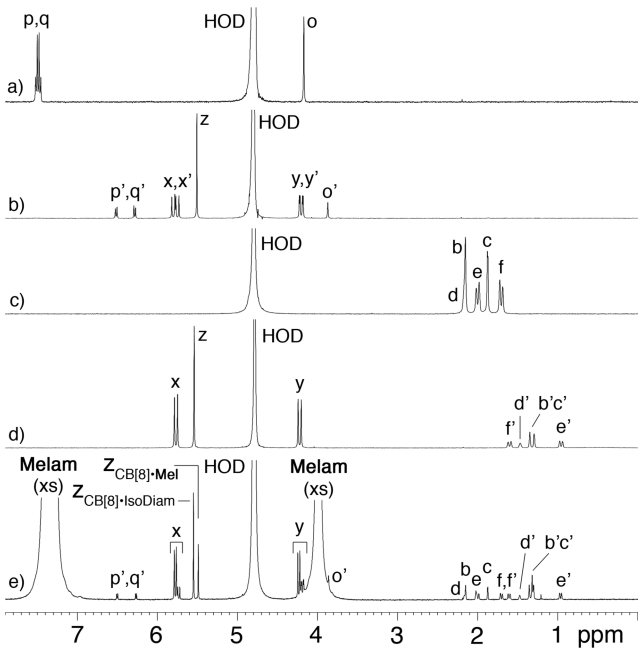

Figure 2. ^{1}H NMR spectra recorded (400 MHz, D_2O, RT) for (a) Melam (0.25 mM), (b) CB[8]·Melam (0.25 mM), (c) IsoDiam-(NH_3)$_2$ (0.25 mM), (d) CB[8]·IsoDiam(NH_3)$_2$, and (e) a competitive mixture of CB[8] (0.2896 mM), IsoDiam(NH_3)$_2$ (0.3248 mM), and Melam (44.64 mM).

plex, and CB[8]·IsoDiam($NHMe_2$)$_2$ in the presence of excess IsoDiam($NHMe_2$)$_2$. Figure 1f establishes that CB[8]·IsoDiam-($NHMe_2$)$_2$ undergoes slow exchange on the ^{1}H NMR time scale with free IsoDiam($NHMe_2$)$_2$, and ^{1}H NMR integration of resonances for IsoDiam($NHMe_2$)$_2$ versus CB[8] in the CB[8]·IsoDiam($NHMe_2$)$_2$ complex establish the 1:1 nature of the host·guest complex. The protons on the diamantane core of IsoDiam($NHMe_2$)$_2$ (H_b–H_e) undergo significant upfield shifts (0.65–0.85 ppm) upon CB[8]·IsoDiam($NHMe_2$)$_2$ complex formation, which establishes cavity binding of the diamantane core. Conversely, the resonances for C(H_a)$_3$ and the axial H_f are substantially less upfield shifted (0.16 and 0.35 ppm), which suggests that these protons are located within the anisotropic shielding region of the cavity but are located near the ureidyl C=O portals. Analysis of related ^{1}H NMR spectra recorded for all of the other complexes shows 1:1 binding with the expected cavity inclusion geometries of the adamantane or diamantane cores of the other guests (Supporting Information).

Measurement of K_{rel} for Competing Pairs of Guests and Calculation of K_a Values for the CB[n]·Guest Complexes. After verifying the 1:1 nature of the CB[n]·guest complexes, we turned our attention to K_a measurements. We employed two different methods to determine the K_a values for the various CB[n]·guest complexes (Table 1). The first method (single-point method)[17] was applied to measure the K_a values for the low affinity host–guest complexes CB[7]·IsoDiam($NHMe_2$)$_2$ (K_a = 686 M^{-1}), CB[7]·IsoDiam(NH_3)$_2$

DOI: 10.1021/jacs.7b00056
J. Am. Chem. Soc. 2017, 139, 3249–3258

Table 1. Binding Constants (K_a, M^{-1}) Measured for the Interaction between CB[7], CB[8], and Various Guests in 50 mM NaOAc Buffer at pH 4.74

	CB[7]	CB[8]
1-AdNH$_3$	(4.2 ± 1.0) × 10^{12} [b]	(8.2 ± 1.8) × 10^{8} [b]
1-AdNH$_2$Et	(8.7 ± 2.0) × 10^{11} [c]	(1.4 ± 0.4) × 10^{9} [e]
1-AdNHEt$_2$	(1.2 ± 0.3) × 10^{11} [c]	(3.1 ± 0.8) × 10^{9} [e]
1-AdNMe$_2$Et	(7.0 ± 1.6) × 10^{11} [c]	(2.8 ± 0.7) × 10^{11} [e]
1-AdNMeEt$_2$	(3.2 ± 0.8) × 10^{11} [c]	(1.1 ± 0.3) × 10^{11} [e]
1-AdNMe$_3$	(1.7 ± 0.4) × 10^{12} [b]	(9.7 ± 2.5) × 10^{10} [b]
1-AdNH$_2$(CH$_2$)$_2$NH$_3$	(2.4 ± 0.6) × 10^{13} [h]	(2.2 ± 0.6) × 10^{10} [e]
1-AdNH$_2$(CH$_2$)$_3$NH$_3$	(1.5 ± 0.4) × 10^{13} [i]	–
1-AdNMe$_2$(CH$_2$)$_3$NH$_3$	(6.8 ± 1.6) × 10^{12} [i]	(1.7 ± 0.4) × 10^{12} [e]
1-AdNHMeCH$_2$CF$_3$	(1.1 ± 0.3) × 10^{11} [c]	(1.3 ± 0.3) × 10^{9} [e]
1-AdNH$_2$CH$_2$CF$_3$	(5.9 ± 1.4) × 10^{11} [c]	(1.0 ± 0.3) × 10^{9} [e]
1-AdPy	(2.0 ± 0.4) × 10^{12} [b]	(2.0 ± 0.5) × 10^{9} [b]
Me$_2$-1-AdNH$_3$	(2.5 ± 0.4) × 10^{4} [b]	(4.3 ± 1.1) × 10^{11} [b]
1,3-Ad(NHMe$_2$)$_2$	(1.2 ± 0.2) × 10^{6} [f]	(1.3 ± 0.3) × 10^{11} [e]
1,3-Ad(NMe$_3$)$_2$	(6.4 ± 1.0) × 10^{4} [b]	(1.1 ± 0.3) × 10^{11} [b]
Me$_2$-1,3-Ad(NHMe$_2$)$_2$	(5.7 ± 0.9) × 10^{5} [f]	–
Me$_2$-1,3-Ad(NMe$_3$)$_2$	(1.8 ± 0.3) × 10^{6} [f]	–
2-AdNH$_3$	(1.3 ± 0.3) × 10^{12} [c]	(6.3 ± 1.6) × 10^{9} [e]
2-AdNMe$_3$	(3.7 ± 0.9) × 10^{12} [c]	(3.6 ± 0.9) × 10^{11} [e]
2,6-Ad(NH$_3$)$_2$	(1.9 ± 0.4) × 10^{12} [i]	(4.7 ± 1.2) × 10^{8} [e]
2,6-Ad(NMe$_3$)$_2$	(3.3 ± 0.9) × 10^{13} [i]	(5.2 ± 1.4) × 10^{10} [g]
Diam(NH$_3$)$_2$	(1.3 ± 0.3) × 10^{11} [h]	(8.3 ± 2.3) × 10^{11} [h]
Diam(NMe$_3$)$_2$	(1.9 ± 0.4) × 10^{15} [h]	(2.0 ± 0.6) × 10^{12} [h]
Diam (NMe$_2$(CH$_2$)$_4$OH)$_2$	(1.9 ± 0.4) × 10^{15} [c]	(1.3 ± 0.3) × 10^{13} [e]
DiamNMe$_3$	(8.0 ± 1.9) × 10^{11} [c]	(2.7 ± 0.7) × 10^{12} [e]
IsoDiam(NH$_3$)$_2$	2030[a]	(3.3 ± 0.8) × 10^{13} [e]
IsoDiam(NHMe$_2$)$_2$	686[a]	(5.7 ± 1.5) × 10^{14} [d]
IsoDiam (NHMe(CH$_2$)$_4$OH)$_2$	194[a]	(9.2 ± 2.4) × 10^{14} [d]
IsoDiamNHMe$_2$	643[a]	(7.8 ± 0.8) × 10^{13} [d]

[a]Measured directly by ^{1}H NMR integration of free and bound guest. [b]Reference 6. Competition experiment used a limiting quantity of CB[n] and [c]1-AdPy, [d]IsoDiam(NH$_3$)$_2$, [e]Melam, [f]TMSP, [g]Me$_2$-1-AdNH$_3$. [h]Reference 9. [i]Reference 11. – = not determined.

(K_a = 2580 M^{-1}), CB[7]·IsoDiam(NHMe(CH$_2$)$_4$OH)$_2$ (K_a = 194 M^{-1}), and CB[7]·IsoDiamNHMe$_2$ (K_a = 643 M^{-1}). Despite the fact that CB[7]·IsoDiam(NHMe$_2$)$_2$ and CB[7]·IsoDiam(NH$_3$)$_2$ are low affinity complexes, they display slow exchange on the ^{1}H NMR time scale, which allows us to separately integrate H$_z$ for free CB[7] and CB[7]·guest. The slow exchange binding is presumably due to the overstuffed nature of the complex and the constrictive nature[18] of the ureidyl C═O portal slowing dissociation. Using the known total concentrations of CB[7] and guest (IsoDiam(NHMe$_2$)$_2$ or IsoDiam(NH$_3$)$_2$) and the mass balance expressions, it is then possible to calculate K_a in the standard way.

The second method, which has been described by us in detail previously,[6,9,10,19] involves competition experiments between a single host (CB[7] or CB[8]), a reference guest of known K_a and a second guest of unknown K_a. Equation 1 shows the equilibrium that we are considering, and eq 2 gives the definition of the relative binding constant K_{rel}. Equations 3–6 present the usual definitions of K_a for the formation of a CB[n]·guest complex. By combining eqs 2, 4, and 6, it is straightforward to demonstrate that K_{rel} is equal to the ratio of K_{a2} to K_{a1} (eq 7). To determine K_{rel}, we monitored these competition experiments by ^{1}H NMR spectroscopy, which takes advantage of the fact that many CB[n]·guest complexes display slow kinetics of exchange on the chemical shift time scale. This allows us to separately integrate peaks for the two competing CB[n]·guest complexes, which, when combined with known total concentrations of CB[n], **G1**, and **G2** and the mass balance expressions, allows us to determine [CB[n]·**G2**], [CB[n]·**G1**], [**G1**], and [**G2**] needed to calculate K_{rel} using eq 2. To be concrete, we illustrate the process for determining K_a for CB[8]·IsoDiam(NH$_3$)$_2$ by competition between CB[8], IsoDiam(NH$_3$)$_2$, and Melam. Figure 2a,b shows the ^{1}H NMR spectra of Melam and CB[8]·Melam, whereas Figure 2c,d shows the spectra for IsoDiam(NH$_3$)$_2$ and CB[8]·IsoDiam-(NH$_3$)$_2$, which allows us to fully identify all of the resonances for the competition experiment between CB[8] (0.2896 mM), IsoDiam(NH$_3$)$_2$ (0.3248 mM), and Melam (44.64 mM) shown in Figure 2e. In this competition experiment, CB[8] is the limiting reagent, tighter binding guest IsoDiam(NH$_3$)$_2$ is used in slight excess, and the concentration of weaker guest Melam is adjusted until comparable amounts of the two competing complexes, CB[8]·IsoDiam(NH$_3$)$_2$ and CB[8]·Melam, are present at equilibrium.

$$\begin{array}{ccc} \text{CB}[n]\cdot\mathbf{G1} & \overset{K_{rel}}{\rightleftharpoons} & \text{CB}[n]\cdot\mathbf{G2} \\ + & & + \\ \mathbf{G2} & & \mathbf{G1} \end{array} \quad (1)$$

$$K_{rel} = \frac{[\text{CB}[n]\cdot\mathbf{G2}][\mathbf{G1}]}{[\text{CB}[n]\cdot\mathbf{G1}][\mathbf{G2}]} \quad (2)$$

$$\text{CB}[n] + \mathbf{G1} \overset{K_{a1}}{\rightleftharpoons} \text{CB}[n]\cdot\mathbf{G1} \quad (3)$$

DOI: 10.1021/jacs.7b00056
J. Am. Chem. Soc. 2017, 139, 3249–3258

$$K_{a1} = \frac{[CB[n]\cdot \mathbf{G1}]}{[CB[n]][\mathbf{G1}]} \quad (4)$$

$$CB[n] + \mathbf{G2} \overset{K_{a2}}{\rightleftharpoons} CB[n]\cdot \mathbf{G2} \quad (5)$$

$$K_{a2} = \frac{[CB[n]\cdot \mathbf{G2}]}{[CB[n]][\mathbf{G2}]} \quad (6)$$

$$K_{rel} = \frac{K_{a2}}{K_{a1}} \quad (7)$$

To ensure that we have reached equilibrium, we performed two complementary experiments: (1) CB[8] and Melam are mixed first to form CB[8]·Melam and then IsoDiam$(NH_3)_2$ is added and (2) CB[8] and IsoDiam$(NH_3)_2$ are mixed first to form CB[8]·IsoDiam$(NH_3)_2$ and then Melam is added. The solutions are separately monitored as a function of time (several weeks in some cases) until equilibrium is established. We separately integrate the resonances for the 16 equivalent equatorial CB[8] protons (H_e) for CB[8]·IsoDiam$(NH_3)_2$ and CB[8]·Melam in the 5.6−5.5 ppm region, which allows us to calculate [CB[8]·IsoDiam$(NH_3)_2$] and [CB[8]·Melam] using the known total concentration of CB[8] and the mass balance expression.[6,9,19] Subsequently, we use the known total concentrations of IsoDiam$(NH_3)_2$ and Melam and the mass balance expressions to calculate [IsoDiam$(NH_3)_2$] and [Melam], which allows a calculation of K_{rel} = 572 for CB[8]·IsoDiam$(NH_3)_2$ versus CB[8]·Melam. Finally, we multiply K_{rel} with the literature value of K_a for CB[8]·Melam (K_a = (5.78 ± 1.36) × 10^{10} M^{-1})[6] to determine K_a for CB[8]·IsoDiam$(NH_3)_2$ as K_a = (3.3 ± 0.8) × 10^{13} (Table 1). In an analogous way, the K_a values for the other CB[n]·guest complexes (Table 1 and Supporting Information) were determined.

Role of Solvation for Binding Affinity Computational Predictions. It is known, that relative solvation energies of small molecules are well reproduced with implicit solvent models such as the conductor-like screening model (COSMO).[20] This class of methods replaces solvent molecules by an electric continuum. In the case of the neutral molecules, a clear distinction has been reported between molecular mechanics (MM)- and quantum mechanics (QM)-based implicit models, showing that those based on the QM electron density are superior to others.[21] However, when comparing neutral, monocationic, and dicationic guests, the situation becomes more complicated.[22] The first successful application of the COSMO method for charged docked guest complexes in CB[7] hosts was reported by Muddana and Gilson.[23]

From the magnitudes of the two main contributions to the ΔG_{calcd}, solvation and interaction energy (see Table S1 in the Supporting Information), it is evident that the accurate description of both terms is of prime importance. Fortunately, it has been shown that in the case of rigid molecules, where the optimized geometry represents both solvated and gas phase conformational ensembles adequately, the implicit solvent models provide reasonable accuracy.[24] These findings greatly simplify important calculations of solvation energies, especially since here the increase of solvation energies from monocationic to dicationic molecule guests is substantial and important.[11]

Discussion of the Trends in Binding Constants Between Hosts CB[7] and CB[8] and the Various Guests. This section is subdivided into a discussion of the binding properties of the 2,6-disubstituted adamantane, 4,9- and 1,6-disubstituted diamantanes, and 1-substituted adamantane derivatives.

2-Substituted Adamantane (Di)ammonium Ions. As described above, we first considered 2,6-disubstituted adamantanes 2,6-Ad$(NH_3)_2$ and 2,6-Ad$(NMe_3)_2$ as potential ultratight binders for CB[n] hosts because of the known tight binding adamantane core, the auspicious five C atom spacing between N atoms, and the potential for ion−dipole interactions at both C═O portals. Previously, we reported that 2,6-Ad$(NH_3)_2$ forms the CB[7]·2,6-Ad$(NH_3)_2$ complex with K_a = (1.9 ± 0.4) × 10^{12} M^{-1}, whereas herein we determine that the corresponding quaternary ammonium ion 2,6-Ad$(NMe_3)_2$ forms a 17-fold stronger complex (CB[7]·2,6-Ad$(NMe_3)_2$; K_a = (3.3 ± 0.9) × 10^{13} M^{-1}).[11,25] When the CB[7]·2,6-Ad$(NMe_3)_2$ K_a value was measured in 2013, it was slightly stronger than the then current record holder (CB[7]·1-Ad$NH_2(CH_2)_2NH_3$, K_a = (2.4 ± 0.6) × 10^{13}), which was gratifying. Similar trends are observed for CB[8], where quaternary diammonium 2,6-Ad$(NMe_3)_2$ (CB[8]·2,6-Ad$(NMe_3)_2$, K_a = (5.2 ± 1.4) × 10^{10} M^{-1}) binds 110-fold tighter than diammonium 2,6-Ad$(NH_3)_2$ does (CB[8]·2,6-Ad$(NH_3)_2$, K_a = (4.7 ± 1.2) × 10^8 M^{-1}). From the literature, it is known that 1-AdNMe_3 binds 2.5-fold more weakly to CB[7] than 1-AdNH_3 does.[6] Accordingly, we wondered why NMe_3^+ groups result in tighter binding in some contexts but not in others.

Disappointingly, diammonium ions 2,6-Ad$(NH_3)_2$ and 2,6-Ad$(NMe_3)_2$ bind only slightly (1.5 and 7.8-fold) stronger to CB[7] than the analogous monoammonium compounds 2-AdNH_3 and 2-AdNMe_3. The 2,6-AdR_2 series of compounds were unable to capture the potential 1000-fold increase in K_a typically obtained for the ion−dipole interaction at an unoccupied CB[n] C═O portal. Even more disappointing was the realization that diammonium ions 2,6-Ad$(NH_3)_2$ and 2,6-Ad$(NMe_3)_2$ bind more weakly to CB[8] than the corresponding monoammonium ions 2-AdNH_3 (CB[8]·2-AdNH_3, K_a = (6.3 ± 1.6) × 10^9 M^{-1}) and 2-AdNMe_3 (CB[8]·2-AdNMe_3, K_a = (3.6 ± 0.9) × 10^{11} M^{-1}) do. Adamantane derived guests 2,6-Ad$(NH_3)_2$ and 2,6-Ad$(NMe_3)_2$ bind substantially stronger to CB[7] (4042-fold and 557-fold) than they do to CB[8], which we attribute to a better match between the size of the adamantane skeleton (cavity volume = 147 $Å^3$) and the cavity of CB[7] (cavity volume = 279 $Å^3$) than to CB[8] (cavity volume = 479 $Å^3$).[4,26]

Previously, we reported the X-ray crystal structures of CB[7]·2,6-Ad$(NH_3)_2$ (CCDC 1444729) and CB[8]·2,6-Ad$(NH_3)_2$ (CCDC 1444821) and used them as an initial geometry for computational work but did not discuss the structures in any detail.[11] In the structure of CB[7]·2,6-Ad$(NH_3)_2$ (Figure 3a), both host and guest occupy a special position of C_2-rotational symmetry in the crystal, which renders both ureidyl C═O portals homotopic. Both N atoms lie approximately in the plane defined by the ureidyl C═O O atoms. The tilt of the C−N bond from the C_7-axis is ≈45° so that an effective hydrogen bond can be formed of 2.932 Å length. There are also two H_2O molecules per portal that provided H-bond bridges between the NH_3^+ groups and the carbonyl O atoms. Figure 3b shows the X-ray crystal structure for CB[8]·2,6-Ad$(NH_3)_2$. Within the crystal, the guest is oriented such that the two ureidyl C═O portals are diastereotopic and both N atoms lie roughly within the plane defined by the C═O O atoms. One NH_3^+ group is directly H-bonded to the ureidyl C═O portal (2.861 Å) along with two additional bridging H_2O molecules. The second NH_3^+ group is roughly centered within the portal with an average

DOI: 10.1021/jacs.7b00056
J. Am. Chem. Soc. 2017, 139, 3249−3258

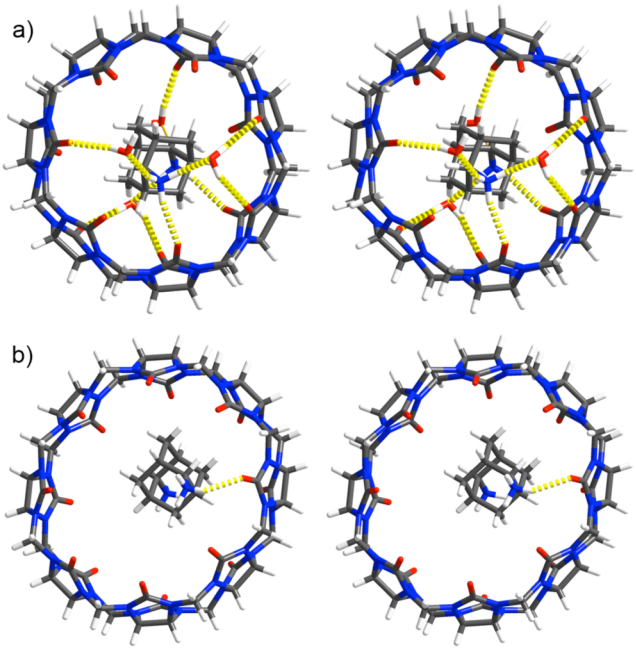

Figure 3. Cross-eyed stereoview representations of the X-ray crystal structures of (a) CB[7]·2,6-Ad(NH_3)$_2$ and (b) CB[8]·2,6-Ad(NH_3)$_2$. Color code: C, gray; H, white; N, blue; O, red; H-bonds, yellow dashes.

$N^+\cdots O{=}C$ distance of 5.0(2) Å. From a comparison of the structures of CB[7]·2,6-Ad(NH_3)$_2$ and CB[8]·2,6-Ad(NH_3)$_2$, it is clear that the 4042-fold reduction in binding affinity is due to the inability of 2,6-Ad(NH_3)$_2$ to completely fill the cavity of CB[8] and displace all high energy water molecules.[8a−c,27] The calculations confirm the better fit of the 2,6-Ad(NH_3)$_2$ guest to CB[7] by increasing the dispersion energy by more than 40% while the electrostatic interaction energy remains the same when compared to that of the larger CB[8] host. Why is the CB[7] complex of diammonium 2,6-Ad(NH_3)$_2$ only 1.5-fold tighter than monoammonium analogue 2-AdNH_3? From the crystal structure of CB[7]·2,6-Ad(NH_3)$_2$, we can speculate that the rigid geometry of 2,6-Ad(NH_3)$_2$ does not allow for a simultaneous optimization of the H-bonding and electrostatic (ion−dipole) interactions at both ureidyl C=O portals. Additionally, the DFT calculations show the profound desolvation (repulsive)−electrostatic energy (attractive) compensation.

Cationic 4,9-Substituted Diamantane Derivatives. Previously, we reported that CB[7] forms a remarkably tight complex with Diam(NMe_3)$_2$ (K_a = (1.9 ± 0.4) × 10^{15} M^{-1}) in sodium acetate buffered D_2O, which we attributed to an optimal N···N spacing (7.8 Å), resulting in 14 nearly ideal $Me_3N^+\cdots O{=}C$ ion−dipole interactions, the hydrophobicity of the diamantane skeleton, and the presence of secondary electrostatic close contacts between the CH_2 groups of the diamantane skeleton of Diam(NMe_3)$_2$ and the C=O groups of CB[7].[9,10] The two NMe_3 groups of Diam(NMe_3)$_2$ are separated by six C atoms, which is known to complement the ≈6.1 Å spacing between ureidyl C=O portals of CB[*n*]. In the X-ray crystal structure of CB[7]·Diam(NMe_3)$_2$, the N atoms of the two NMe_3 groups are located 0.80 Å above the center of the plane defined by the ureidyl carbonyl O atoms (Figure 4a). Diam(NH_3)$_2$, which lacks the quaternary ammonium centers, binds ≈14 600-fold more weakly; this highlights the importance

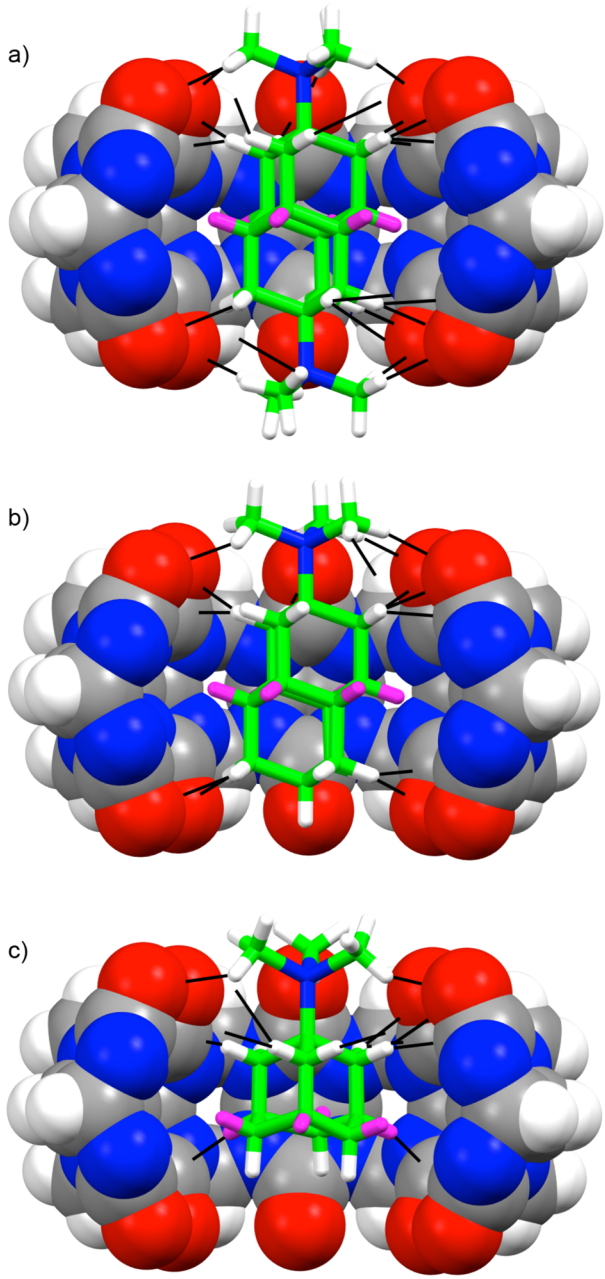

Figure 4. Cutaway representations rendered from the X-ray crystal structures of (a) CB[7]·Diam(NMe_3)$_2$, (b) CB[7]·DiamNMe_3, and (c) CB[7]·1-AdNMe_3. Color code for CB[7]: C, gray; H, white; N, blue; O, red. Color code for guests: C, green; N, blue; H, white; equatorial H on central cyclohexane ring, purple. H···O and H···C close contacts, black lines.

of the $Me_3N^+\cdots O{=}C$ interactions toward the binding. Additionally, this exceptionally tight fit is manifested by the largest dispersion energy contribution to the binding energy among all tested complexes.

To further refine our understanding of the structural features of Diam(NMe_3)$_2$ that promoted ultratight binding—especially the location of the NMe_3 groups from the C=O portal plane—we prepared and studied monocationic analogue DiamNMe_3 and also re-examined the binding of the CB[7]·1-AdNMe_3 complex. We found that the CB[7]·DiamNMe_3 complex (K_a = 8.0 × 10^{11} M^{-1}) is 2375-fold weaker than CB[7]·Diam(NMe_3)$_2$ due to the loss of ion−dipole inter-

DOI: 10.1021/jacs.7b00056
J. Am. Chem. Soc. 2017, 139, 3249−3258

actions at the second ureidyl C═O portal (computationally accompanied by decreases in the dispersion and electrostatic energy by 9 and 43 kcal/mol, i.e., 12 and 41%, respectively); this energetic penalty for the deletion of ion−dipole interactions at one C═O portal is in line with previous research in the CB[*n*] field.[8a,12] Figure 4a−c shows the X-ray crystal structures of CB[7]·Diam$(NMe_3)_2$, CB[7]·DiamNMe$_3$, and CB[7]·1-AdNMe$_3$. The geometrical features of the structures of CB[7]·Diam$(NMe_3)_2$ and CB[7]·DiamNMe$_3$ are very similar; for example, (1) the long axis of the DiamNMe$_3$ is aligned with the C_7-axis of CB[7], (2) the equatorial planes of CB[7] and the central cyclohexyl unit (C−H bonds colored purple) of DiamNMe$_3$ are roughly coplanar and coincident, (3) most of the CH_2 groups of the diamantane skeleton of DiamNMe$_3$ exhibit close contacts (less than the sum of the van der Waals radii) with the ureidyl C═O portals O atoms, and (4) the Me_3N N atom is located 0.78 Å above the mean plane of the C═O O atoms in the CB[7]·DiamNMe$_3$ complex.

We were also able to obtain the X-ray crystal structure for CB[7]·1-AdNMe$_3$ (Figure 4c). Intriguingly, for CB[7]·1-AdNMe$_3$, the Me_3N N atom is *only* 0.32 Å above the mean plane of the C═O O atoms, and the corresponding cyclohexane ring of 1-AdNMe$_3$ (C−H bonds colored purple) averages 0.43 Å *below* the equatorial plane of CB[7]. The deeper penetration of 1-AdNMe$_3$ into CB[7] implies that the 0.78−0.80 Å Me_3N to portal plane distance for CB[7]·DiamNMe$_3$ and CB[7]·Diam$(NMe_3)_2$ does not optimize ion−dipole interactions. The DFT calculations confirmed this observation. On the basis of the structural evidence, it appears that the noncovalent close contacts between guest diamantane CH_2 groups and host C═O O atoms at each portal and the location of the equatorial cyclohexane C−H bonds of DiamNMe$_3$ and Diam$(NMe_3)_2$ in the wider equatorial plane of CB[7] enforce the observed geometries. In turn, this suggests that rigid diammonium guests scaffolds that enforce a 0.32 Å Me_3N^+ to portal distance may exhibit binding constants that exceed that of CB[7]·Diam$(NMe_3)_2$.

We also obtained the X-ray crystal structure of the isomeric CB[7]·2-AdNMe$_3$ (Supporting Information) in which the N atom of the NMe$_3$ group is 0.442 Å above the plane defined by the ureidyl C═O O atoms. As a route to achieve even higher binding affinity, we studied Diam$(NMe_2(CH_2)_4OH)_2$, which was obtained as a synthetic byproduct that has two side arms that feature OH groups that might undergo additional OH···O═C H-bonding interactions. In practice, we measured K_a = (1.9 ± 0.4) × 10^{15} M^{-1} for CB[7]·Diam$(NMe_2(CH_2)_4OH)_2$, which is identical to that measured for CB[7]·Diam$(NMe_3)_2$. The X-ray crystal structure of CB[7]·Diam$(NMe_2(CH_2)_4OH)_2$ (Supporting Information) provides a clear explanation in that the OH side arm is not H-bonded to the C═O portal in the crystal, probably because of steric shielding provided by the quaternary ammonium ion at the portal.

Cationic 1,6-Substituted Diamantane Derivatives. Next, we synthesized the medial 1,6-disubstituted diamantane compounds, which are isomeric to the 4,9-disubstituted derivatives but feature a four carbon atom spacing between cationic N atoms and a lateral rather than longitudinal distribution of their steric bulk.[13a] In this article, we studied the binding properties of CB[7] and CB[8] toward IsoDiam-$(NH_3)_2$, IsoDiam$(NHMe_2)_2$, IsoDiam$(NHMe(CH_2)_4OH)_2$, and IsoDiamNHMe$_2$ as a monocationic model compound (Table 1).

The contrasts between the Diam and IsoDiam series are striking. Whereas the Diam compounds are tight binders for both CB[7] and CB[8] (10^{11} to 10^{15} M^{-1} range), the IsoDiam compounds bind weakly to CB[7] with K_a values in the 10^2 to 10^3 M^{-1} range. The 14-carbon atom IsoDiam skeleton is too wide and voluminous[8a] to be encapsulated inside CB[7] without engendering substantial host·guest strain, which decreases the net binding free energy. A similar phenomenon has been observed previously for Me_2-1-AdNH$_3$.[6] Accordingly, the selectivity of the IsoDiam compounds for CB[8] over CB[7] is quite remarkable. For example, the CB[7]·IsoDiam-$(NHMe_2)_2$ complex (K_a = 686 M^{-1}) is ≈10^{12}-fold weaker than the CB[8]·IsoDiam$(NHMe_2)_2$ complex (K_a = (5.7 ± 1.5) × 10^{14} M^{-1}). Unlike in the Diam series, the monocationic control complex CB[8]·IsoDiamNHMe$_2$ (K_a = (7.8 ± 0.8) × 10^{13} M^{-1}) binds only 7-fold weaker than its dicationic analogue CB[8]·IsoDiam$(NHMe_2)_2$. The increase of dispersion energy here (by 22%) seems to be marginal when compared to a 100% increase of electrostatic energy even when one does take into account the larger solvation penalty. The primary diammonium complex CB[8]·IsoDiam$(NH_3)_2$ is 17-fold weaker than CB[8]·IsoDiam$(NHMe_2)_2$, which again shows that N-methylation plays a significant role in the system; unfortunately, the corresponding quaternary ammonium salts were synthetically inaccessible, as described previously.[13a]

These CB[8]·IsoDiam complexes are also noteworthy for their absolute binding affinity, which is in the 10^{13} to 10^{14} M^{-1} range. Previously, Scherman and Nau suggested that CB[7] optimizes the energy content of encapsulated water molecules (e.g., number and energy) relative to CB[6] and CB[8] and that it should be the strongest binder in the CB[*n*] series.[8b] The present findings establish that CB[8] should be considered closely alongside CB[7] as an ultratight binding host. Additionally, this is supported by the fact that reported total energies of high energy water molecules inside of the CB[7] and CB[8] species are close (when the uncertainty is taken into account) and is in essential agreement with the water map results reported recently.[11]

The X-ray crystal structures of CB[8]·IsoDiam$(NH_3)_2$ and CB[8]·IsoDiam$(NHMe_2)_2$ are shown in Figure 5. In both

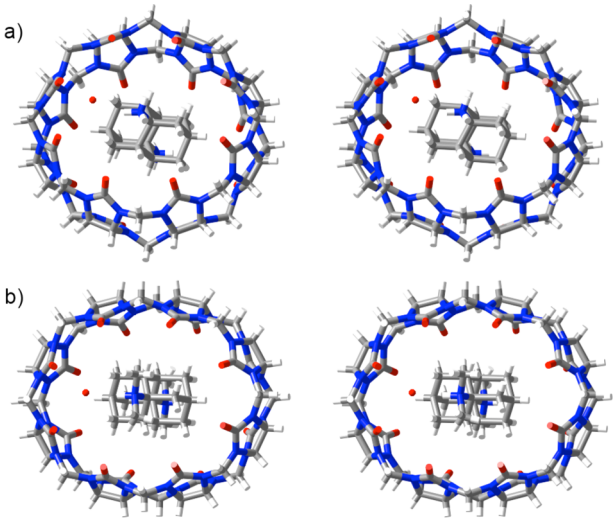

Figure 5. Cross-eyed stereoview representations of the X-ray crystal structures of (a) CB[8]·IsoDiam$(NH_3)_2$ and (b) CB[8]·IsoDiam-$(NHMe_2)_2$. Color code: C, gray; H, white; N, blue; O, red.

DOI: 10.1021/jacs.7b00056
J. Am. Chem. Soc. 2017, 139, 3249−3258

cases, the long axis of the IsoDiam skeleton is encapsulated inside the CB[8] cavity, which positions the cationic residues at the portal. To accommodate the ≈6.6 Å width of the IsoDiam skeleton, the CB[8] macrocycles undergoes an ellipsoidal deformation (CB[8]·IsoDiam(NH_3)$_2$: 13.10 × 12.17 Å; CB[8]·IsoDiam($NHMe_2$)$_2$: 13.59 × 11.49 Å). Quite interestingly, because of the lateral steric bulk of the IsoDiam skeleton, the ammonium ions within CB[8]·IsoDiam(NH_3)$_2$ and CB[8]·IsoDiam($NHMe_2$)$_2$ do not display direct H-bonding with the C═O portals. For example, the N···O═C distances in CB[8]·IsoDiam(NH_3)$_2$ range from 4.61 to 5.22 Å, which are well beyond H-bonding distances. Instead, one water molecule acts as a bridge between guest and host. Ion−dipole interactions mediated by the CH_3 groups are observed for CB[8]·IsoDiam($NHMe_2$)$_2$, with four CH_3N^+···O═C distances in the 4.456−4.638 Å range (Figure 5b). These additional ion−dipole interactions help to explain the 17-fold increase in affinity observed for CB[8]·IsoDiam($NHMe_2$)$_2$.

Within the IsoDiam series, the most tightly bound complex is CB[8]·IsoDiam(NHMe(CH_2)$_4$OH)$_2$, with K_a = (9.2 ± 2.4) × 10^{14} M^{-1}. It is tempting to suggest that the slight increase in affinity observed relative to CB[8]·IsoDiam($NHMe_2$)$_2$ is due to loop formation via H-bonding between the side arm OH group and the regions of the C═O portal not fully engaged in ion−dipole interactions, and DFT calculations (Supporting Information) support this hypothesis. These analyses suggest that future studies should be aimed at preparing IsoDiam compounds with cationic arms to fully capitalize on the negative electrostatic potential of the uncomplexed portions of the ureidyl C═O portals of CB[8].

1-Substituted Adamantane (Di)ammonium Ions. As part of our study of the diamantane derivatives, we often had occasion to test certain hypotheses using the synthetically more accessible adamantane skeleton. In this section, we describe the influence of fluorination, looping, alkylation, and steric bulk.

Influence of Fluorination. As described above, the presence of numerous N^+CH_2···O═C ion−dipole interactions plays an important role in the ultratight complex CB[7]·Diam(NMe_3)$_2$. Accordingly, we considered the addition of an electronegative substituent (e.g., fluorinated) that would enhance the ion−dipole interaction by making the involved CH_2 groups more electropositive. We synthesized 1-Ad$NH_2CH_2CF_3$ and 1-AdNHMeCH_2CF_3 and measured their binding constants toward CB[7] and CB[8] (Table 1) to test this hypothesis. We found that 1-AdNH_2Et and 1-Ad$NH_2CH_2CF_3$ bind to CB[7] (8.7 × 10^{11} and 5.9 × 10^{11} M-1) and CB[8] (1.4 × 10^9 and 1.0 × 10^9 M^{-1}) with comparable affinity. Comparison between 1-AdNHMeCH_2CF_3 and 1-Ad$NHEt_2$ revealed similarly minor differences in binding affinity. We conclude that the presence of CF_3 substituents in this system is ineffective at increasing K_a via stronger ion−dipole interactions. Recently, Masson has successfully demonstrated a related subtle effect using aryl substituted derivatives of $Me_3SiCH_2NH_2CH_2Ph$.[28]

Influence of Looping Interactions. The potential to increase the affinity of CB[*n*]·guest complexes by the addition of primary ammonium ion arms (e.g., butanediammonium versus spermine) was recognized as early as the pioneering work of Mock[12] and has been employed more recently in the context of CB[7]·guest complexes by Kim and Inoue and by Ghosh and Isaacs and has been shown to be moderately effective.[7c,8d,29] For example, CB[6] binds 9.7-fold more tightly to spermine than spermidine, which in turn binds 8.8-fold more tightly than butanediammonium.[12] Similarly, CB[7] binds 10-fold more strongly to TMSAA than to TMSA.[9] We refer to this as a *primary ammonium looping strategy* since the anchoring ammonium ion is primary and the added ammonium ion arm is intended to loop from one part of the C═O portal to an adjacent portion. In a combined computational and experimental paper, we recently reported the binding constants for CB[7]·1-Ad$NH_2(CH_2)_2NH_3$, CB[7]·1-Ad$NH_2(CH_2)_3NH_3$, and CB[7]·1-Ad$NMe_2(CH_2)_3NH_3$, which are included in Table 1, shedding additional light on the effectiveness of looping.[11] For example, both 1-Ad$NH_2(CH_2)_2NH_3$ (5.6-fold) and 1-Ad$NH_2(CH_2)_3NH_3$ (3.6-fold) bind more tightly to CB[7] than 1-AdNH_3. The length of the loop is directly proportional to deformation energy required to make the loop reach back, which in turn weakens the binding. In this article, we newly measured binding constants for 1-Ad$NH_2(CH_2)_2NH_3$ and 1-Ad$NMe_2(CH_2)_3NH_3$ toward CB[8]. Interestingly, we found that the primary ammonium looping strategy is more effective with CB[8], where the CB[8]·1-Ad$NH_2(CH_2)_2NH_3$ complex is 27-fold tighter than CB[8]·1-AdNH_3. Similarly, comparison of 1-AdNMe_3 with 1-Ad$NMe_2(CH_2)_3NH_3$ allowed us to previously assess the effectiveness of *quaternary ammonium looping* with CB[7].[11] We found that the CB[7]·1-Ad$NMe_2(CH_2)_3NH_3$ complex (K_a = 6.8 × 10^{12} M^{-1}) was 4-fold stronger than the CB[7]·1-AdNMe_3 complex. In contrast, from our newly measured binding constants toward CB[8], we found that the CB[8]·1-Ad$NMe_2(CH_2)_3NH_3$ complex (K_a = 1.7 × 10^{12} M^{-1}) is 18-fold stronger than CB[8]·1-AdNMe_3. This result indicates that quaternary looping is more effective with CB[8] than CB[7], presumably because the larger electrostatically negative C═O portal of CB[8] is only *locally* neutralized by a monoammonium ion.

Influence of Alkylation State. The large difference in binding affinity sometimes observed between primary ammonium (e.g., Diam(NH_3)$_2$) and quaternary ammonium ions (e.g., Diam(NMe_3)$_2$) led us to investigate the influence of alkylation state on affinity within the 1-Ad series. For example, across the series from CB[7]·1-AdNH_3 (K_a = 4.2 × 10^{12} M^{-1}) to CB[7]·1-AdNH_2Et (K_a = 8.7 × 10^{11} M^{-1}) to CB[7]·1-Ad$NHEt_2$ (K_a = 1.2 × 10^{11} M^{-1}), the binding affinity decrease stepwise 4.8-fold and 7.3-fold. We believe this effect reflects the decrease in the number of NH···O═C H-bonds and steric effects due to the larger Et substituents. A related 5.3-fold (probably steric) decrease in binding constant is seen along the CB[7]·1-AdNMe_3 to CB[7]·1-AdNMe_2Et to CB[7]·1-Ad$NMeEt_2$ series. The trend for the larger CB[8] is reversed, where K_a values increase 3.8-fold along the CB[8]·1-AdNH_3 to CB[8]·1-AdNH_2Et to CB[8]·1-Ad$NHEt_2$. Overall, the effect of the number and identity of alkyl groups on binding constant is small relative to the driving force provided by the hydrophobic effect and ion−dipole interactions.

Influence of Steric Bulk. From previous studies,[13d] three compounds were available in the 1,3-AdR_2 and Me_2-1,3-AdR_2 series that were complementary to the CB[*n*]·1,3-Ad(NMe_3)$_2$ complexes studied previously. All four compounds exhibit low binding constants toward CB[7] because the size of all four guests exceeds the strain free capacity of CB[7]. However, it is noted that the CB[7]·1,3-Ad($NHMe_2$)$_2$ complex (K_a = 1.2 × 10^6 M^{-1}) is 19-fold stronger than CB[7]·1,3-Ad(NMe_3)$_2$, which is clearly related the reduction in steric demand of the ammonium ion that is inside the CB[7] cavity.[6] Overall, the influence of steric bulk on equilibrium binding constant is

DOI: 10.1021/jacs.7b00056
J. Am. Chem. Soc. 2017, 139, 3249−3258

relatively straightforward to assess based on molecular modeling.

CONCLUSIONS

In summary, we have studied the interaction of four series of guests (2,6-disubstituted adamantanes, 4,9-disubstituted diamantanes, 1,6-disubstituted diamantanes, and 1-substituted adamantanes) with CB[7] and CB[8] by a combination of ^{1}H NMR spectroscopy, X-ray crystallography, and molecular modeling. Although the CB[7]·2,6-Ad(NMe_3)$_2$ complex (K_a = 3.3 × 10^{13} M^{-1}) bested the affinity of CB[7]·1-Ad$NH_2(CH_2)_2NH_3$, it did not capture the 1000-fold increase in K_a expected. Accordingly, we turned to the Diam and IsoDiam systems and discovered the tightest binding host·guest pair (CB[7]·Diam(NMe_3)$_2$) currently known in the CB[7]·guest literature.

Comparative crystallographic studies among CB[7]·Diam(NMe_3)$_2$, CB[7]·DiamNMe_3, and CB[7]·1-AdNMe_3 reveals that $^+NMe_3$ groups naturally position themselves ≈0.32 Å above the mean plane of the ureidyl C═O portals to optimize ion−dipole interactions. The observed geometrical features of CB[7]·Diam(NMe_3)$_2$ and CB[7]·DiamNMe_3 (0.78 and 0.80 Å above C═O portals) reflect the constraints imposed by the close contacts between CH_2 groups on Diam and the ureidyl C═O groups of CB[7].

On the basis of the energy content of the encapsulated high energy water molecules, Scherman and Nau previously suggest that CB[7] would be the tightest binding host in the CB[n] family.[8b] We were surprised, therefore, to find that the CB[8]·IsoDiam(NHMe$(CH_2)_4$OH)$_2$ (K_a = 9.2 × 10^{14} M^{-1}) reaches comparable levels of affinity to CB[7]·Diam(NMe_3)$_2$ (K_a = 1.9 × 10^{15} M^{-1}). This can be explained by fact that the difference in total energy of high energy water molecules inside of the CB[7] and CB[8] species is close within the uncertainty of reported values and WaterMap calculations.

Finally, we studied the CB[n]·1-Ad series and documented the following: (1) a larger effect of a primary or quaternary ammonium looping strategy on the CB[8]·guest binding constant (18−27-fold increase) and (2) relatively small effects of alkyl group identity and alkyl group fluorination upon the observed K_a values. Future studies aim to take advantage of the ability of the larger portals of CB[8] to better capture ion−dipole interactions via a looping strategy to create CB[8]·guest complexes to establish CB[8] as the ultratight binder in the CB[n]·guest series. Overall, the work deepens our knowledge of the factors governing high affinity binding in CB[n]·guest complexes and provides strategies to tune host·guest recognition processes for specific applications including as an alternative for avidin·biotin in biotechnology applications.

ASSOCIATED CONTENT

Supporting Information

The Supporting Information is available free of charge on the ACS Publications website at DOI: 10.1021/jacs.7b00056.

Synthetic procedures and characterization for all new compounds, ^{1}H NMR binding studies, ^{1}H NMR competition experiments for K_a determination, computational methods, and correlation between experimental and calculated ΔG (PDF)

Crystallographic information file for CB[7]·1-AdNMe_3 (CIF)

Crystallographic information file for CB[7]·2-AdNMe_3 (CIF)

Crystallographic information file for CB[7]·DiamNMe_3 (CIF)

Crystallographic information file for CB[7]·Diam-($NMe_2(CH_2)_4OH)_2$ (CIF)

Crystallographic information file for CB[8]·IsoDiam-($NH_3)_2$ (CIF)

Crystallographic information file for CB[8]·IsoDiam-($NHMe_2)_2$ (CIF)

AUTHOR INFORMATION

Corresponding Authors

*pavel.hobza@marge.uochb.cas.cz (P.H.)

*majerski@irb.hr (K.M.-M.)

*glaser.robert@gmail.com (R.G.)

*LIsaacs@umd.edu (L.I.)

ORCID

Marina Šekutor: 0000-0003-1629-3672

Lyle Isaacs: 0000-0002-4079-332X

Notes

The authors declare no competing financial interest.

ACKNOWLEDGMENTS

We thank the National Science Foundation (CHE-1404911 to L.I.), the Croatian Ministry of Science, Education, and Sports (grant 098-0982933-2911 to K.M.-M.), the Croatian Academy of Sciences and Arts (K.M.-M. and M.Š.), and the Ben-Gurion Univ. Scientific Relations Research Fund (R.G.) for financial support. This work was also supported by research project RVO 61388963 awarded to the Institute of Organic Chemistry and Biochemistry, Academy of Sciences of the Czech Republic, the Czech Science Foundation (grant number P208/12/G016) and by project L01305 of the Ministry of Education, Youth and Sports of the Czech Republic.

REFERENCES

(1) (a) Green, N. M. *Methods Enzymol.* **1990**, *184*, 51−67. (b) Wilchek, M.; Bayer, E. A. *Methods Enzymol.* **1990**, *184*, 14−45. (c) Laitinen, O. H.; Nordlund, H. R.; Hytoenen, V. P.; Kulomaa, M. S. *Trends Biotechnol.* **2007**, *25*, 269−277. (d) Ostojic, G. N.; Hersam, M. C. *Small* **2012**, *8*, 1840−1845.

(2) (a) Peck, E. M.; Liu, W.; Spence, G. T.; Shaw, S. K.; Davis, A. P.; Destecroix, H.; Smith, B. D. *J. Am. Chem. Soc.* **2015**, *137*, 8668−8671. (b) Liu, W.; Peck, E. M.; Smith, B. D. *J. Phys. Chem. B* **2016**, *120*, 995−1001.

(3) (a) Freeman, W. A.; Mock, W. L.; Shih, N.-Y. *J. Am. Chem. Soc.* **1981**, *103*, 7367−7368. (b) Kim, J.; Jung, I.-S.; Kim, S.-Y.; Lee, E.; Kang, J.-K.; Sakamoto, S.; Yamaguchi, K.; Kim, K. *J. Am. Chem. Soc.* **2000**, *122*, 540−541. (c) Day, A. I.; Arnold, A. P.; Blanch, R. J.; Snushall, B. *J. Org. Chem.* **2001**, *66*, 8094−8100. (d) Day, A. I.; Blanch, R. J.; Arnold, A. P.; Lorenzo, S.; Lewis, G. R.; Dance, I. *Angew. Chem., Int. Ed.* **2002**, *41*, 275−277. (e) Liu, S.; Zavalij, P. Y.; Isaacs, L. *J. Am. Chem. Soc.* **2005**, *127*, 16798−16799. (f) Cheng, X.-J.; Liang, L.-L.; Chen, K.; Ji, N.-N.; Xiao, X.; Zhang, J.-X.; Zhang, Y.-Q.; Xue, S.-F.; Zhu, Q.-J.; Ni, X.-L.; Tao, Z. *Angew. Chem., Int. Ed.* **2013**, *52*, 7252−7255.

(4) Lee, J. W.; Samal, S.; Selvapalam, N.; Kim, H.-J.; Kim, K. *Acc. Chem. Res.* **2003**, *36*, 621−630.

(5) Mock, W. L.; Shih, N.-Y. *J. Org. Chem.* **1986**, *51*, 4440−4446.

(6) Liu, S.; Ruspic, C.; Mukhopadhyay, P.; Chakrabarti, S.; Zavalij, P. Y.; Isaacs, L. *J. Am. Chem. Soc.* **2005**, *127*, 15959−15967.

(7) (a) Jeon, W. S.; Moon, K.; Park, S. H.; Chun, H.; Ko, Y. H.; Lee, J. Y.; Lee, E. S.; Samal, S.; Selvapalam, N.; Rekharsky, M. V.; Sindelar,

DOI: 10.1021/jacs.7b00056
J. Am. Chem. Soc. 2017, 139, 3249−3258

V.; Sobransingh, D.; Inoue, Y.; Kaifer, A. E.; Kim, K. *J. Am. Chem. Soc.* **2005**, *127*, 12984−12989. (b) Rekharsky, M. V.; Mori, T.; Yang, C.; Ko, Y. H.; Selvapalam, N.; Kim, H.; Sobransingh, D.; Kaifer, A. E.; Liu, S.; Isaacs, L.; Chen, W.; Moghaddam, S.; Gilson, M. K.; Kim, K.; Inoue, Y. *Proc. Natl. Acad. Sci. U. S. A.* **2007**, *104*, 20737−20742. (c) Moghaddam, S.; Yang, C.; Rekharsky, M.; Ko, Y. H.; Kim, K.; Inoue, Y.; Gilson, M. K. *J. Am. Chem. Soc.* **2011**, *133*, 3570−3581. (d) Kaifer, A. E.; Li, W.; Yi, S. *Isr. J. Chem.* **2011**, *51*, 496−505. (e) Assaf, K. I.; Ural, M. S.; Pan, F.; Georgiev, T.; Simova, S.; Rissanen, K.; Gabel, D.; Nau, W. M. *Angew. Chem., Int. Ed.* **2015**, *54*, 6852−6856.

(8) (a) Nau, W. M.; Florea, M.; Assaf, K. I. *Isr. J. Chem.* **2011**, *51*, 559−577. (b) Biedermann, F.; Uzunova, V. D.; Scherman, O. A.; Nau, W. M.; De Simone, A. *J. Am. Chem. Soc.* **2012**, *134*, 15318−15323. (c) Biedermann, F.; Nau, W. M.; Schneider, H.-J. *Angew. Chem., Int. Ed.* **2014**, *53*, 11158−11171. (d) Rekharsky, M. V.; Ko, Y.-H.; Selvapalam, N.; Kim, K.; Inoue, Y. *Supramol. Chem.* **2007**, *19*, 39−46. (e) Shetty, D.; Khedkar, J. K.; Park, K. M.; Kim, K. *Chem. Soc. Rev.* **2015**, *44*, 8747−8761. (f) Nguyen, C. N.; Kurtzman Young, T.; Gilson, M. K. *J. Chem. Phys.* **2012**, *137*, 044101.

(9) Cao, L.; Šekutor, M.; Zavalij, P. Y.; Mlinarić-Majerski, K.; Glaser, R.; Isaacs, L. *Angew. Chem., Int. Ed.* **2014**, *53*, 988−993.

(10) (a) Cao, L.; Škalamera, D.; Zavalij, P. Y.; Hostaš, J.; Hobza, P.; Mlinarić-Majerski, K.; Glaser, R.; Isaacs, L. *Org. Biomol. Chem.* **2015**, *13*, 6249−6254. (b) Škalamera, D.; Cao, L.; Isaacs, L.; Glaser, R.; Mlinarić-Majerski, K. *Tetrahedron* **2016**, *72*, 1541−1546.

(11) Hostaš, J.; Sigwalt, D.; Šekutor, M.; Ajani, H.; Dubecký, M.; Řezáč, J.; Zavalij, P. Y.; Cao, L.; Wohlschlager, C.; Mlinarić-Majerski, K.; Isaacs, L.; Glaser, R.; Hobza, P. *Chem. - Eur. J.* **2016**, *22*, 17226−17238.

(12) Mock, W. L.; Shih, N.-Y. *J. Am. Chem. Soc.* **1988**, *110*, 4706−4710.

(13) (a) Šekutor, M.; Molčanov, K.; Cao, L.; Isaacs, L.; Glaser, R.; Mlinarić-Majerski, K. *Eur. J. Org. Chem.* **2014**, *2014*, 2533−2542. (b) Glaser, R.; Steinberg, A.; Šekutor, M.; Rominger, F.; Trapp, O.; Mlinarić-Majerski, K. *Eur. J. Org. Chem.* **2011**, *2011*, 3500−3506. (c) Lucas, D.; Minami, T.; Iannuzzi, G.; Cao, L.; Wittenberg, J. B.; Anzenbacher, P.; Isaacs, L. *J. Am. Chem. Soc.* **2011**, *133*, 17966−17976. (d) Ergaz, I.; Toscano, R. A.; Delgado, G.; Steinberg, A.; Glaser, R. *Cryst. Growth Des.* **2008**, *8*, 1399−1405.

(14) Bush, M. E.; Bouley, N. D.; Urbach, A. R. *J. Am. Chem. Soc.* **2005**, *127*, 14511−14517.

(15) (a) Marquez, C.; Hudgins, R. R.; Nau, W. M. *J. Am. Chem. Soc.* **2004**, *126*, 5806−5816. (b) Jeon, Y.-M.; Kim, J.; Whang, D.; Kim, K. *J. Am. Chem. Soc.* **1996**, *118*, 9790−9791. (c) Buschmann, H. J.; Cleve, E.; Schollmeyer, E. *Inorg. Chim. Acta* **1992**, *193*, 93−97.

(16) (a) Masson, E.; Ling, X.; Joseph, R.; Kyeremeh-Mensah, L.; Lu, X. *RSC Adv.* **2012**, *2*, 1213−1247. (b) Barrow, S. J.; Kasera, S.; Rowland, M. J.; del Barrio, J.; Scherman, O. A. *Chem. Rev.* **2015**, *115*, 12320−12406.

(17) Connors, K. A. *Binding Constants*; John Wiley & Sons: New York, 1987.

(18) (a) Marquez, C.; Nau, W. M. *Angew. Chem., Int. Ed.* **2001**, *40*, 3155−3160. (b) Quan, M. L. C.; Cram, D. J. *J. Am. Chem. Soc.* **1991**, *113*, 2754−2755.

(19) Cao, L.; Isaacs, L. *Supramol. Chem.* **2014**, *26*, 251−258.

(20) Klamt, A.; Schüürmann, G. *J. Chem. Soc., Perkin Trans. 2* **1993**, 799−805.

(21) Kolář, M.; Fanfrlík, J.; Lepšík, M.; Forti, F.; Luque, F. J.; Hobza, P. *J. Phys. Chem. B* **2013**, *117*, 5950−5962.

(22) Lepšík, M.; Řezáč, J.; Kolář, M.; Pecina, A.; Hobza, P.; Fanfrlík, J. *ChemPlusChem* **2013**, *78*, 921−931.

(23) Muddana, H. S.; Gilson, M. K. *J. Chem. Theory Comput.* **2012**, *8*, 2023−2033.

(24) Mennucci, B. *J. Phys. Chem. Lett.* **2010**, *1*, 1666−1674.

(25) In ref 11, we erroneously reported the K_a for CB[7]·2,6-Ad$(NH_3)_2$ as 1.2×10^{12} M^{-1} due to a typographical error. The value of $K_a = 1.9 \times 10^{12}$ M^{-1} reported herein is correct.

(26) Nau, W. M.; Florea, M.; Assaf, K. I. *Isr. J. Chem.* **2011**, *51*, 559−577.

(27) Biedermann, F.; Vendruscolo, M.; Scherman, O. A.; De Simone, A.; Nau, W. M. *J. Am. Chem. Soc.* **2013**, *135*, 14879−14888.

(28) Ling, X.; Saretz, S.; Xiao, L.; Francescon, J.; Masson, E. *Chem. Sci.* **2016**, *7*, 3569−3573.

(29) Ghosh, S.; Isaacs, L. *J. Am. Chem. Soc.* **2010**, *132*, 4445−4454.

DOI: 10.1021/jacs.7b00056
J. Am. Chem. Soc. 2017, 139, 3249−3258